National Research Centre **“Kurchatov Institute”**

A.A. Logunov INSTITUTE FOR HIGH ENERGY PHYSICS
of the National Research Centre “Kurchatov Institute”

Single-spin asymmetry in the reaction $p^{\uparrow} + A(p) \rightarrow \pi^{0} X$

V.V. Abramov, IHEP, Protvino

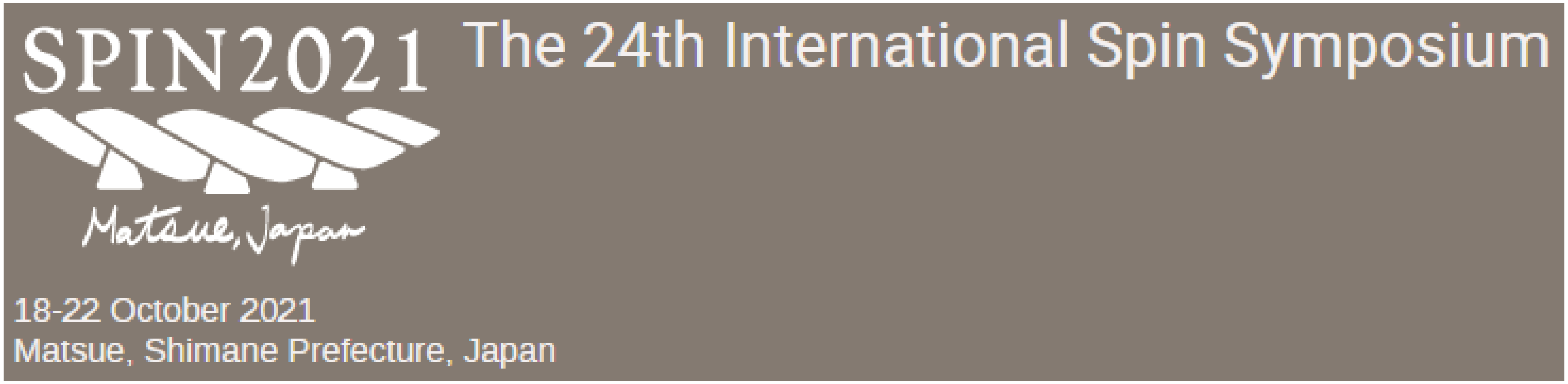

October 20, 2021

Talk content

1. Introduction

2. The Chromo-magnetic polarization of quarks (CPQ) model

3. Existing data for $A_N(x_F, p_T)$ in $p\uparrow + p(A) \rightarrow \pi^0 + X$

4. The CPQ model predictions for $A_N(x_F, p_T)$ in $p\uparrow + p(A) \rightarrow \pi^0 + X$

5. Conclusions and outlook

Introduction

The single-spin asymmetry (A_N) of π^0 - mesons in the collisions of polarized protons with protons and nuclei has been studied in many experiments in a wide range of energies and other kinematic variables. Recently, data on nuclear targets have appeared, which provide additional information on the mechanism of single-spin effects.

There are special areas of A_N dependence on various variables, where A_N can reach extremely large values, either change sign, or exhibit an oscillating dependence on x_F. A global analysis of the single-spin data (including 87 inclusive reactions) within the framework of the model of chromomagnetic polarization of quarks (CPQ) makes it possible to single out such areas and plan the corresponding measurements to verify the performed calculations and thereby advance in the study of the mechanism of single-spin effects.

Model of chromomagnetic polarization of quarks (CPQ)

The CPQ model assumes that a circular transverse chromomagnetic field $\mathbf{B}^a$ exists in the interaction region. It is created by relativistic spectator quarks moving forward and backward in the c.m. $\boldsymbol{\mu}^a_Q = \mathbf{s} g^a g_s / 2M_Q$ – the chromomagnetic dipole moment of the constituent quark Q interacts with the inhomogeneous chromomagnetic field and Stern-Gerlach force arises. The Stern-Gerlach force acts on the test quark (which will be a part of the detected hadron) and gives it a p_T kick to the left or right for the quark spin directed UP or DN. The field gradient has the same direction to the left and right relative to the collision axis, which provides a non-zero polarization effect.

The precession of the quark spin in the chromomagnetic field $\mathbf{B}^a$ changes the components of the Stern-Gerlach force, which leads to oscillation of P_N or A_N, depending on their arguments (x_F, p_T) in the case of a sufficiently strong field $\mathbf{B}^a$ [1,2]. In the CPQ model, the interaction region can be considered in the c.m. frame as a microscopic Stern-Gerlach apparatus (see Fig. 1 below):

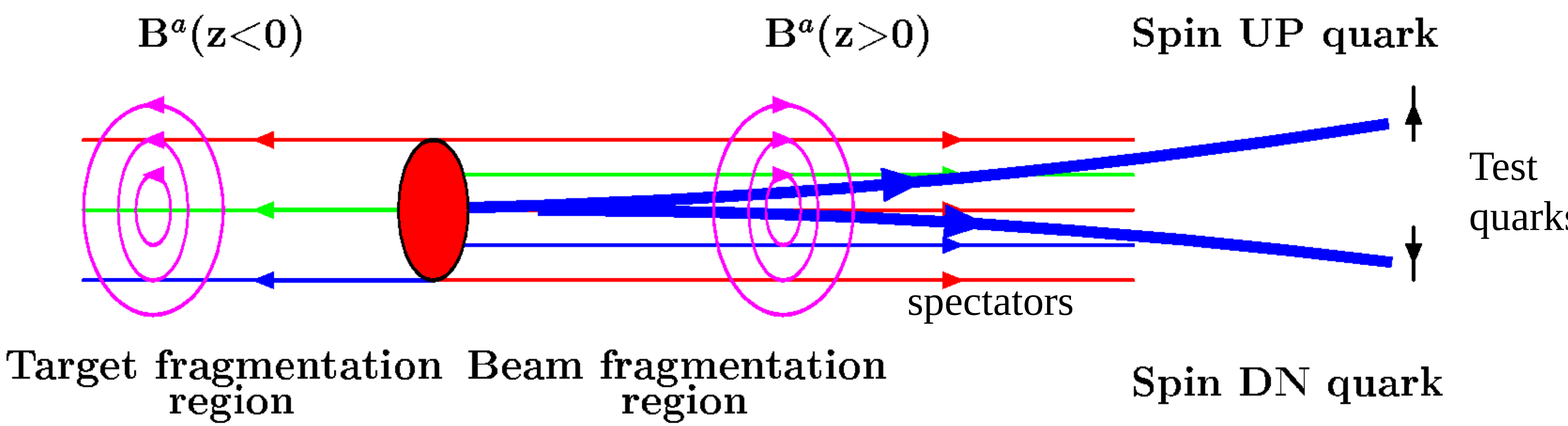

Fig. 1

Dependence of A_N on atomic weight (A) and energy ($\sqrt{s}$)

In the CPQ model the number of spectator quarks which create the effective chromomagnetic field $\mathbf{B^a}$ depend on the reaction type, $\sqrt{s}$ and A. The number of spectator quarks depends on $\sqrt{s}$ due to production at high energies additional $\tilde{q}q$-pairs. $\mathbf{f_N}$ is number of $\tilde{q}q$-pairs per one valence quark in the projectile and in the target and it grows with increasing $\sqrt{s}$. The contribution of new quarks $\mathbf{f_N(\sqrt{s}, p_T, x_F)}$ to the field $\mathbf{B^a}$ is suppressed at large p_T and x_F, since the fast test quark is ahead of the spectator quarks and the field they create has no influence on it. The dependence on A is given by

$$\mathbf{A_{eff} \approx 0.69A^{1/3}}. \qquad (1)$$

We assume that in pA-collisions the effective numbers of quarks ($\mathbf{q_A}$) and antiquarks ($\mathbf{\tilde{q}_A}$) in the incident baryon ($A=A_1$) or target nucleus ($A=A_2$) are given by a set of equations:

$$\mathbf{q_A = 3(1 + f_N)A_{eff}, \quad \tilde{q}_A = 3f_NA_{eff},} \qquad (2)$$

where $\mathbf{f_N = n_q exp(-W/\sqrt{s})(1 - x_N)^n, \;\; x_N = [(p_T/p_N)^2 + x_F{}^2]^{1/2}, \;\; n_q = 4.22 \pm 0.08,} \qquad (3)$

$$\mathbf{W = W_0/(A_1A_2)^{1/6}, \quad n = (A_1A_2)^{1/6}, \quad W_0 = 267.0 \pm 3.7\ GeV \approx M_p{}^2/m_q;} \qquad (4)$$

$$\mathbf{p_N = p_{N0}(A_1A_2)^{-2\alpha/3}; \; \alpha = 0.0350 \pm 0.0017; \;\; p_{N0} = 75.0 \pm 15.0\ GeV/c;} \qquad (5)$$

$\mathbf{m_q = (m_u + m_d)/2 \approx 3\ MeV}$ – average current mass of light **u** and **d** quarks.

Quark spin precession in the color field

$\boldsymbol{ds/dt} \approx a[\mathbf{s}\, \mathbf{B}^a]$ (F-T-BMT-equation) (6)

$a = g_s(g^a_Q - 2 + 2M_Q/E_Q)/2M_Q$, $g_s = \pm\sqrt{(4\pi\alpha_s)}$ – color quark charge (7)

Constituent quark masses $M_U \approx M_D \approx 0.3$ GeV, E_Q – quark energy in c.m.

$\boldsymbol{\Delta\mu^a_Q = (g^a_Q - 2)/2 < 0}$ (quark anomalous chromomagnetic moment). (8)

At $E_Q = 2M_Q/(2-g^a_Q) = -M_Q/\Delta\mu^a_Q$, $\boldsymbol{ds/dt = 0}$. **Prediction: There is usually a local maximum of $A_N(\sqrt{s})$ around $\sqrt{s} = E_R \approx 4M_Q/(2-g^a_Q) = -2M_Q/\Delta\mu^a_Q$.** (9).

Prediction: Ocsillation of $A_N(x_F)$ and $P_N(x_F)$ in the case of a strong B^a field.

- Due to the spontaneous breaking of chiral symmetry appear the $\Delta M_Q(q) \approx 0.3$ GeV and $\Delta\mu^a_Q(q)$ of the constituent quarks, where q – momentum transfer.

In the instanton model: $\boldsymbol{\Delta\mu^a_Q}(0) \approx \boldsymbol{-0.4}$ **(N. Kochelev); [3]** (10)

Model-dependent (CPQ) estimate of $\boldsymbol{\Delta\mu^a_Q}$ for u,d,s,c,b-quarks were obtained from the global analysis of polarization data, including 87 reactions:

- $\boldsymbol{\Delta\mu^a_Q}$ (u,c) $\boldsymbol{= -0.4839 \pm 0.0017}$, q=+2/3; (11)
- $\boldsymbol{\Delta\mu^a_Q}$ (d,s,b) $\approx \boldsymbol{\sqrt{(2/3)}\, \Delta\mu^a_Q(u,c)}$, q=-1/3. (12)

Existing data on $A_N(x_F, p_T)$ for $p\uparrow + p(A) \rightarrow \pi^0 + X$

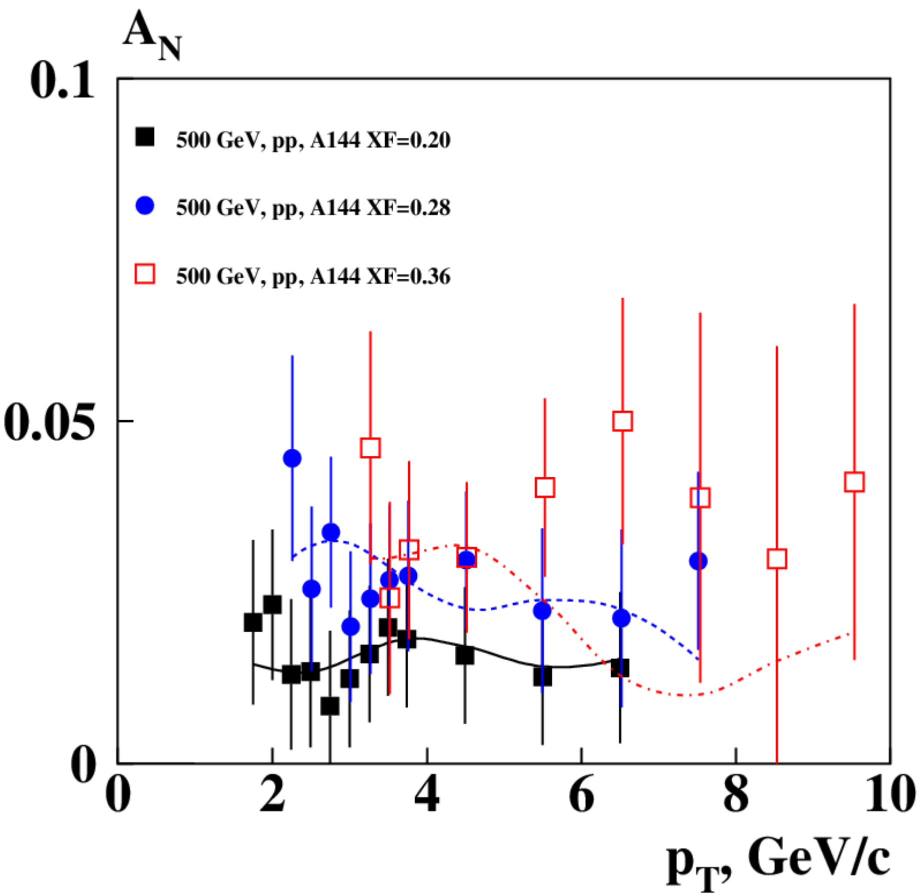

Fig. 2. Dependence of A_N on p_T at energy in c.m. $\sqrt{s}$ = 500 GeV and for several values of x_F in pp collisions [4].

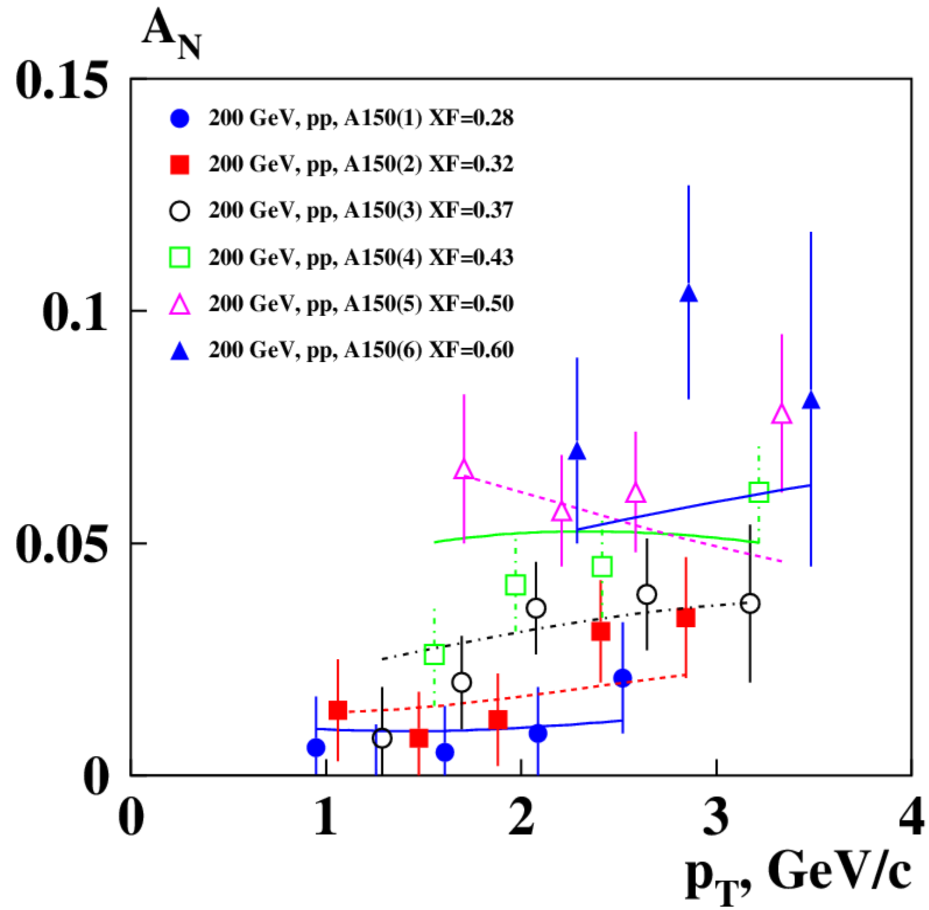

Fig. 3. Dependence of A_N on p_T at energy $\sqrt{s}$ = 200 GeV and for several values of x_F in pp collisions [5].

Curves show calculations using the CPQ model. The CPQ model is consistent with the data. No decrease in $A_N(p_T)$ with increasing p_T, as predicted by the pQCD, is observed.

Existing data on $A_N(x_F, p_T)$ for $p\uparrow + p(A) \rightarrow \pi^0 + X$

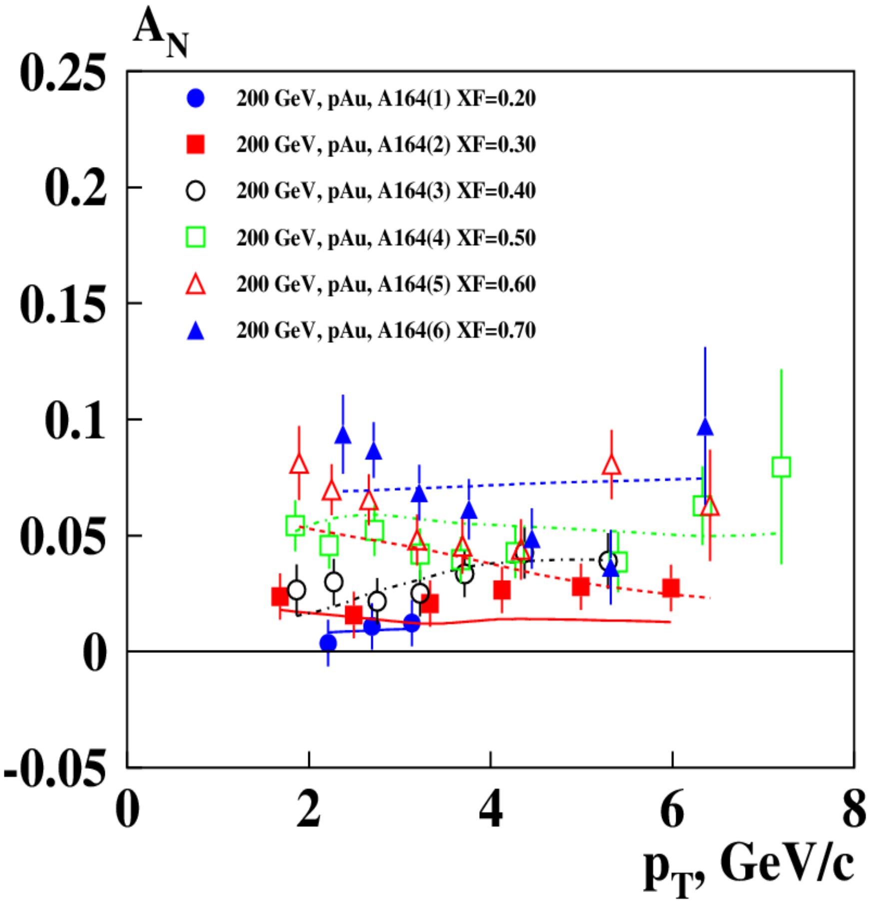

Fig. 4. Dependence of A_N on p_T at energy $\sqrt{s}$ = 200 GeV and for several values of x_F in pAu collisions [6].

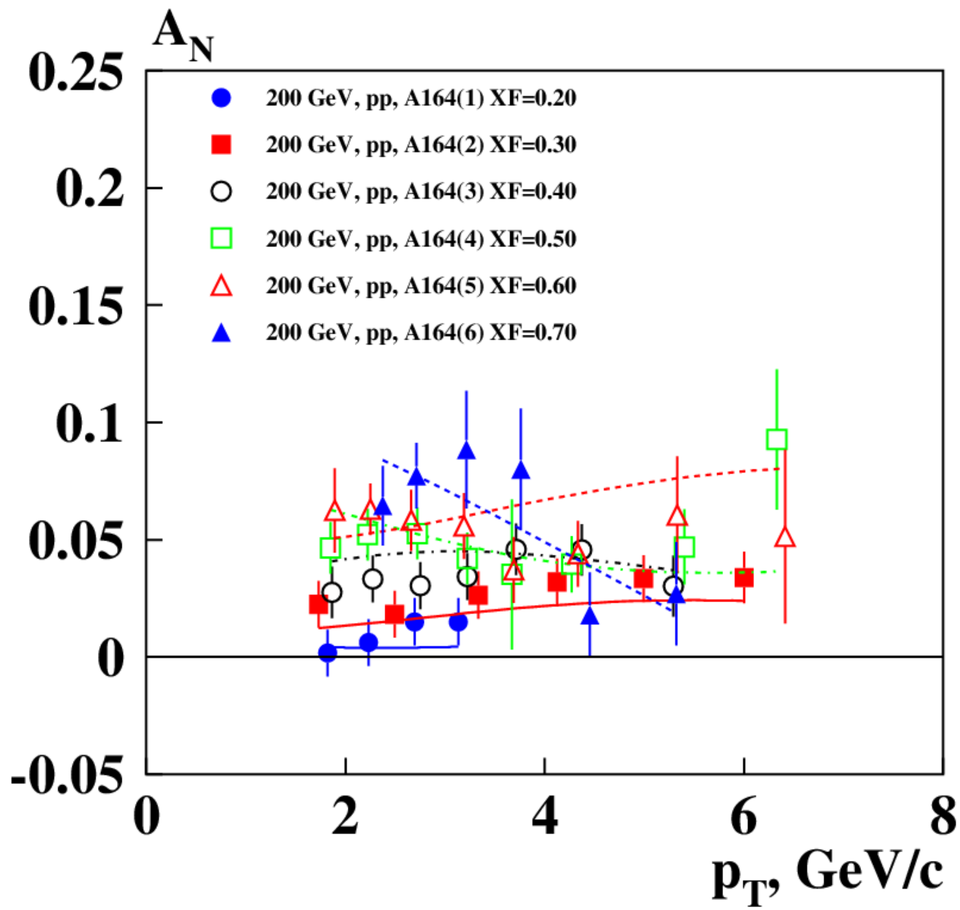

Fig. 5. Dependence of A_N on p_T at energy $\sqrt{s}$ = 200 GeV and for several values of x_F in pp collisions [6].

The CPQ model is consistent with the data. There is a weak A-dependence of A_N.

Existing data on $A_N(x_F, p_T)$ for $p\uparrow + p(A) \rightarrow \pi^0 + X$

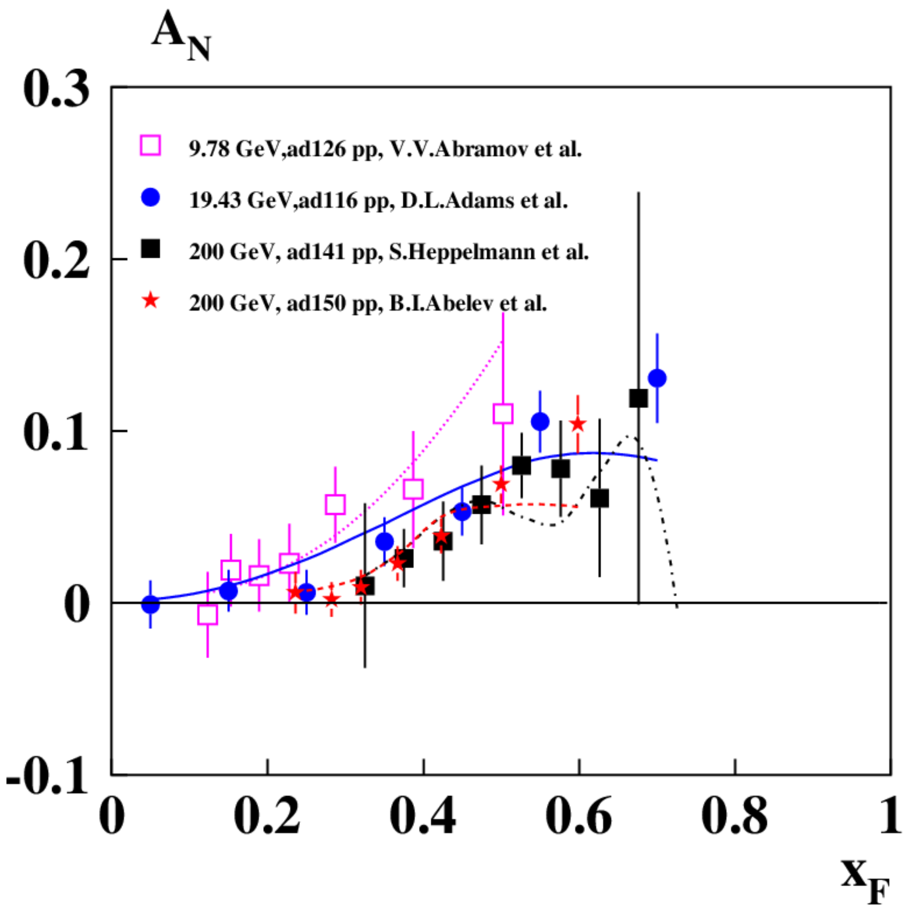

Fig. 6. Dependence of A_N on x_F at energies $\sqrt{s}$ = 9.78, 19.43 and 200 GeV in pp collisions [7,8,9,5].

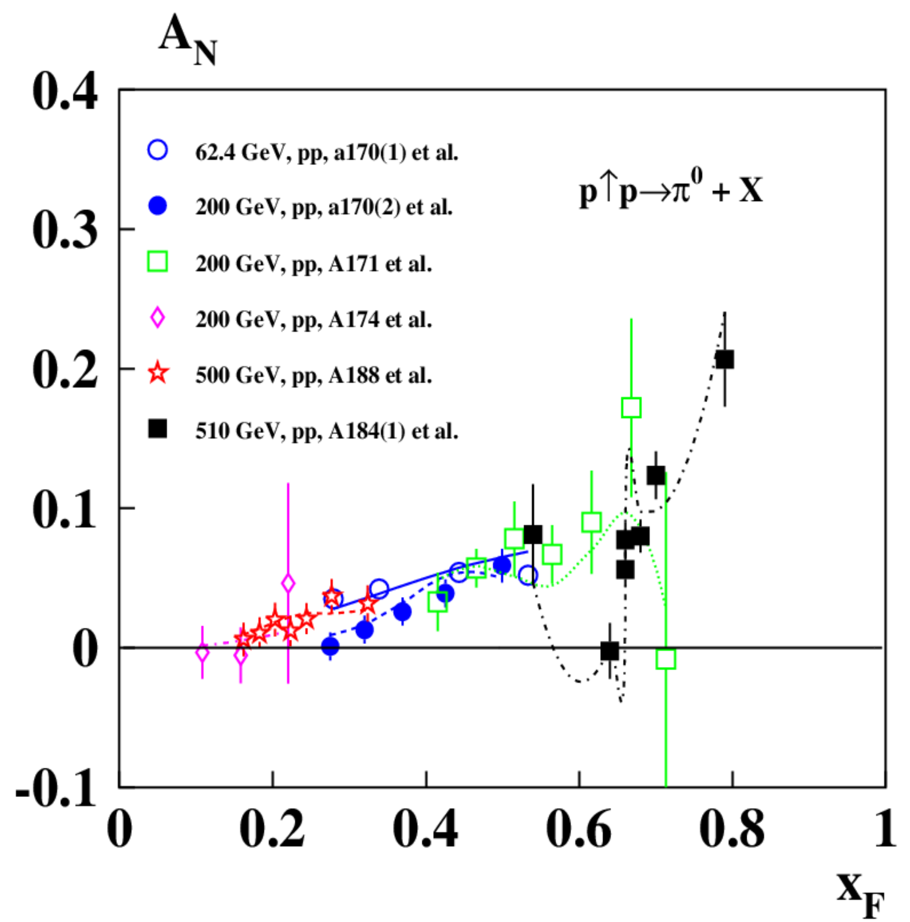

Fig. 7. Dependence of A_N on x_F at energies $\sqrt{s}$ = 62.4 [10], 200 [10,11,12], 500 [13] and 510 [14] GeV in pp collisions.

$A_N(x_F,\sqrt{s})$ is usually rising with x_F. Some dependence of A_N on $\sqrt{s}$ is visible.

Predictions on $A_N(x_F, p_T)$ for $p\uparrow + p(A) \rightarrow \pi^0 + X$

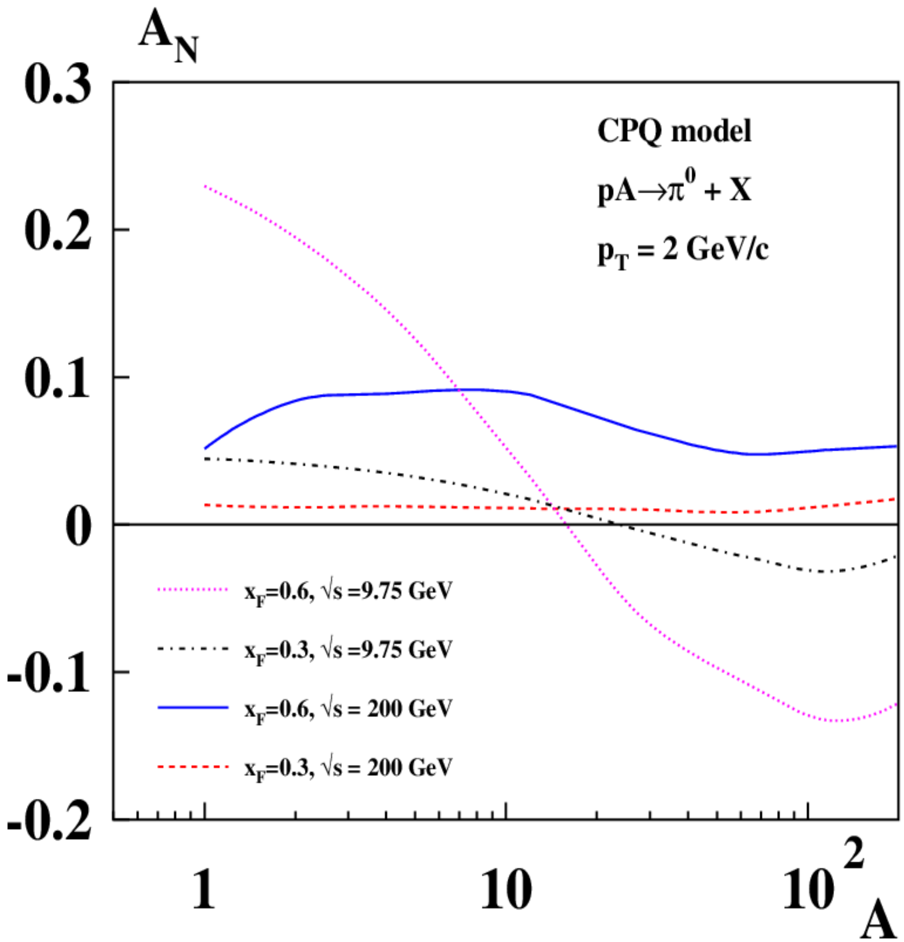

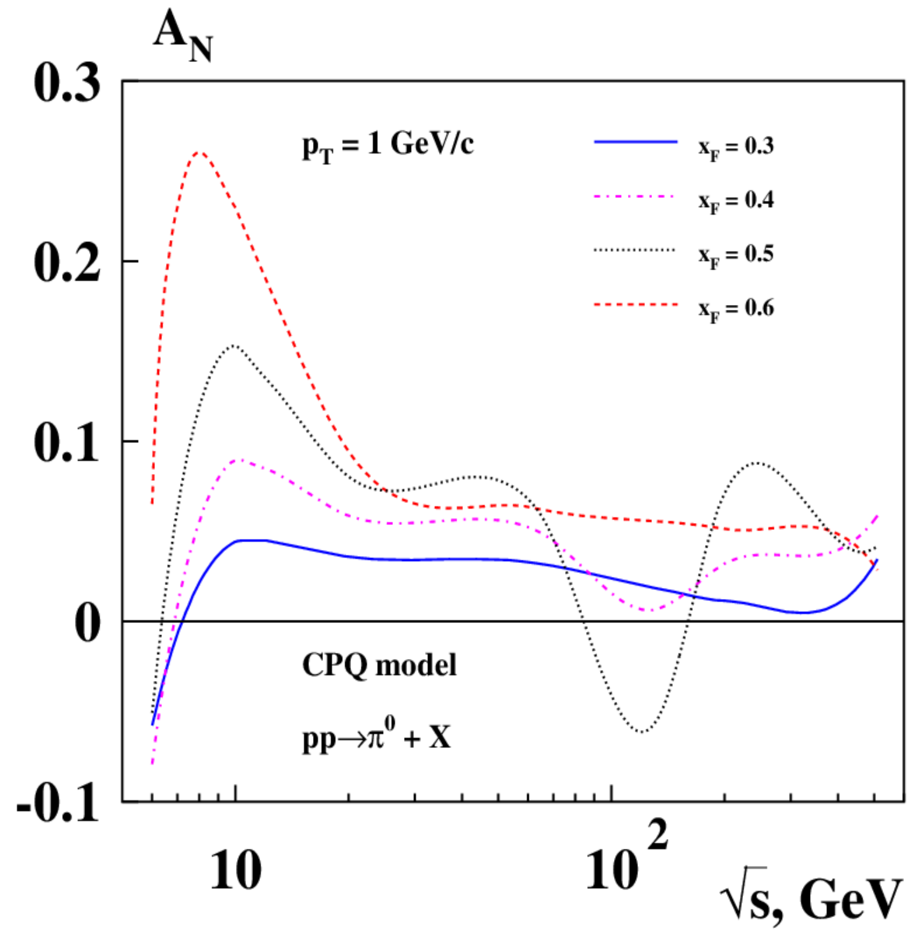

Fig. 8. Calculations of the dependence of A_N on A at energies $\sqrt{s}$ = 9.75 and 200 GeV in pA collisions.

Fig. 9. Calculations of the dependence of A_N on the energy $\sqrt{s}$ for several values of x_F in pp collisions.

Strong $A_N(A)$ dependence at $\sqrt{s}$ = 9.75 GeV and x_F=0.6. Negative $A_N(\sqrt{s})$ at $\sqrt{s}$ = 130 GeV and x_F=0.5. Large positive $A_N(\sqrt{s})$ at $\sqrt{s}$ =9.75 GeV and x_F=0.6.

Predictions on $A_N(x_F, p_T)$ for $p\uparrow + p(A) \to \pi^0 + X$

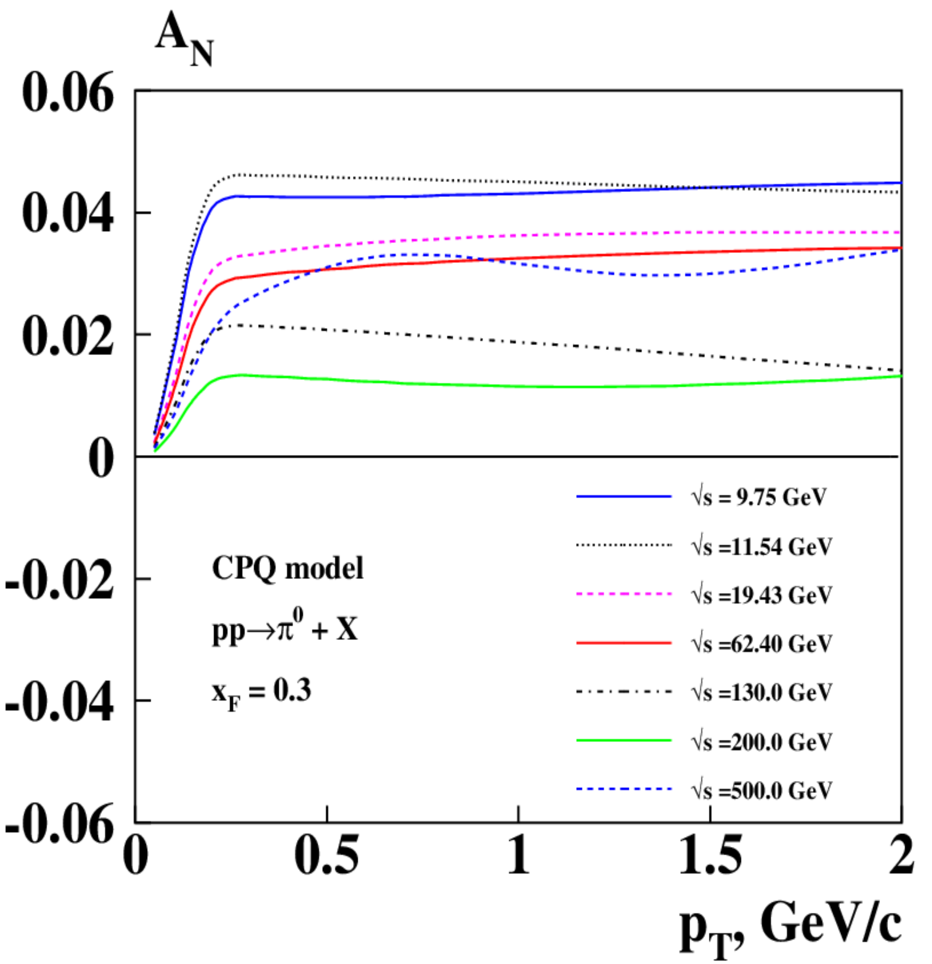

Fig. 10. Calculations of the dependence of A_N on p_T for several values of energy $\sqrt{s}$, at $x_F = 0.3$, in pp-collisions.

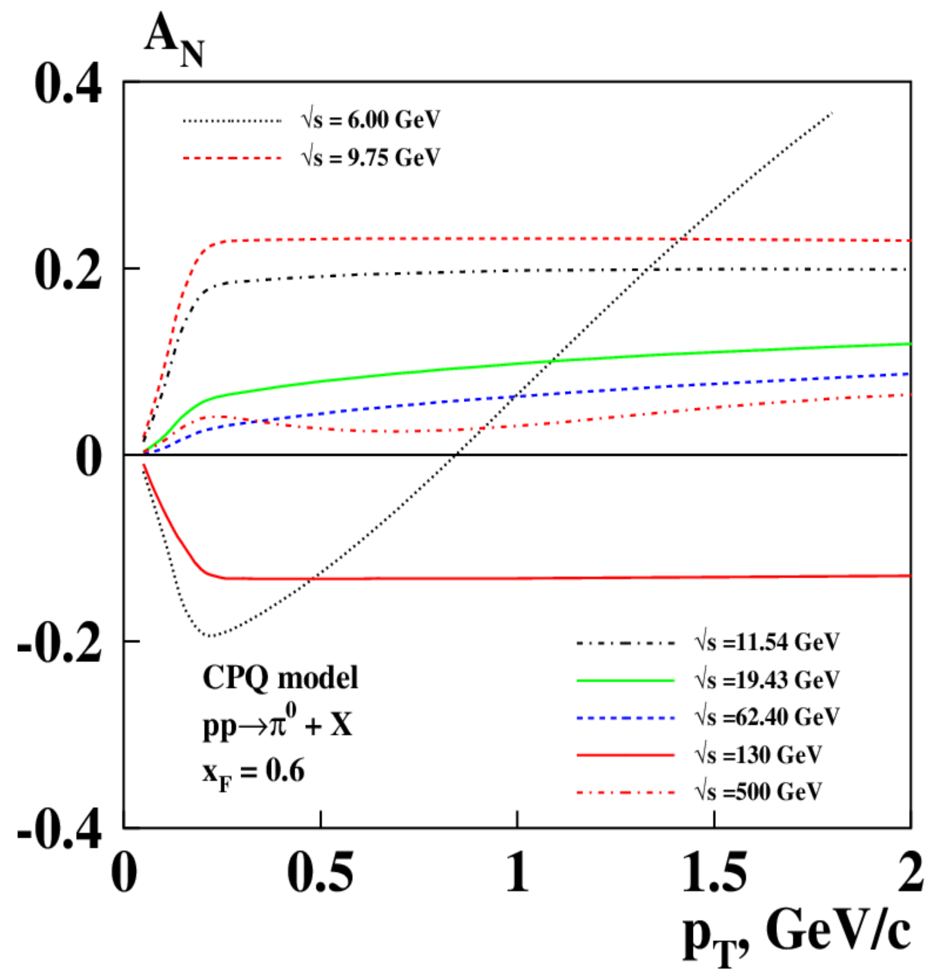

Fig. 11. Calculations of the dependence of A_N on p_T for several values of energy $\sqrt{s}$, at $x_F = 0.6$, in pp collisions.

Plane $A_N(p_T)$ dependence at $p_T > 0.3$ GeV/c, $\sqrt{s} > 9$ GeV.

Predictions on $A_N(x_F, p_T)$ for $p\uparrow + p(A) \longrightarrow \pi^0 + X$

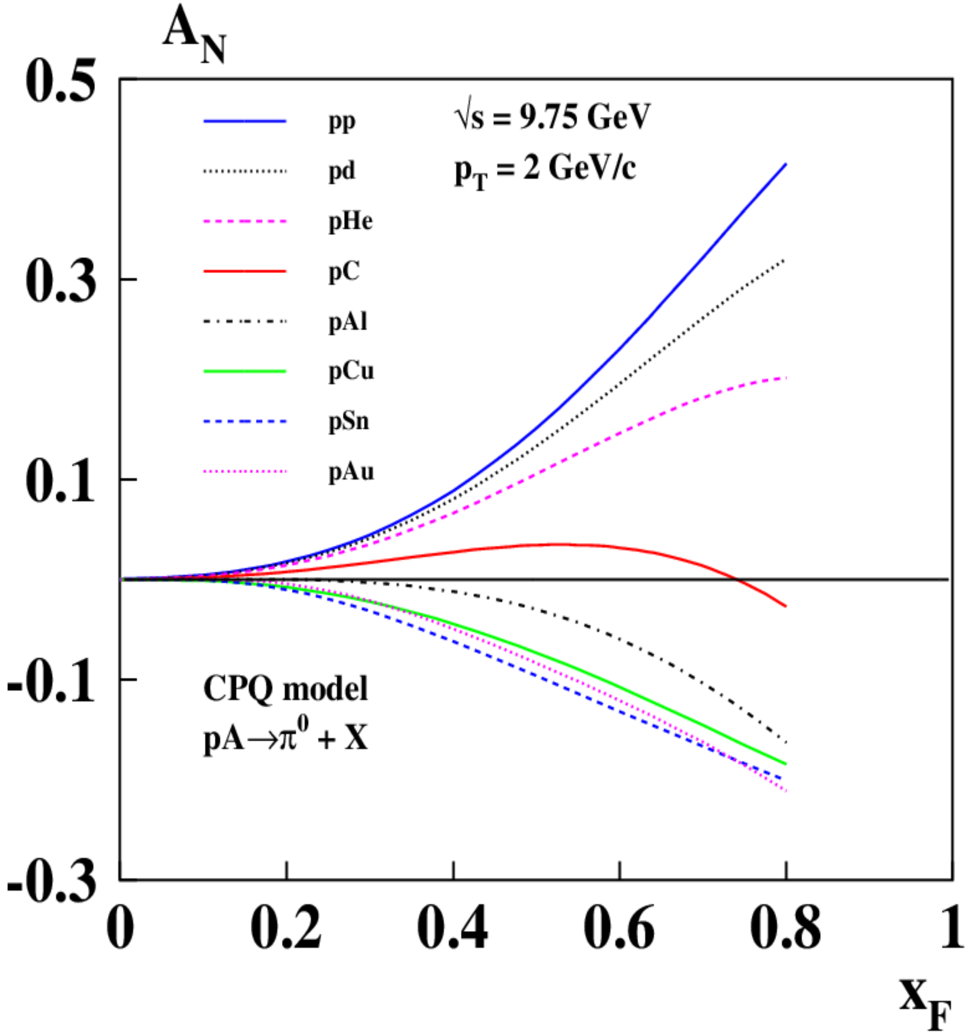

Fig. 12. Calculations of the dependence of A_N on x_F at energy $\sqrt{s}$ = 9.75 GeV, p_T = 2 GeV / c, in pA collisions.

Strong dependence of $A_N(x_F, A)$ on A at high x_F at $\sqrt{s}$ = 9.75 GeV.

Predictions on $A_N(x_F, p_T)$ for $p\uparrow + p(A) \rightarrow \pi^0 + X$

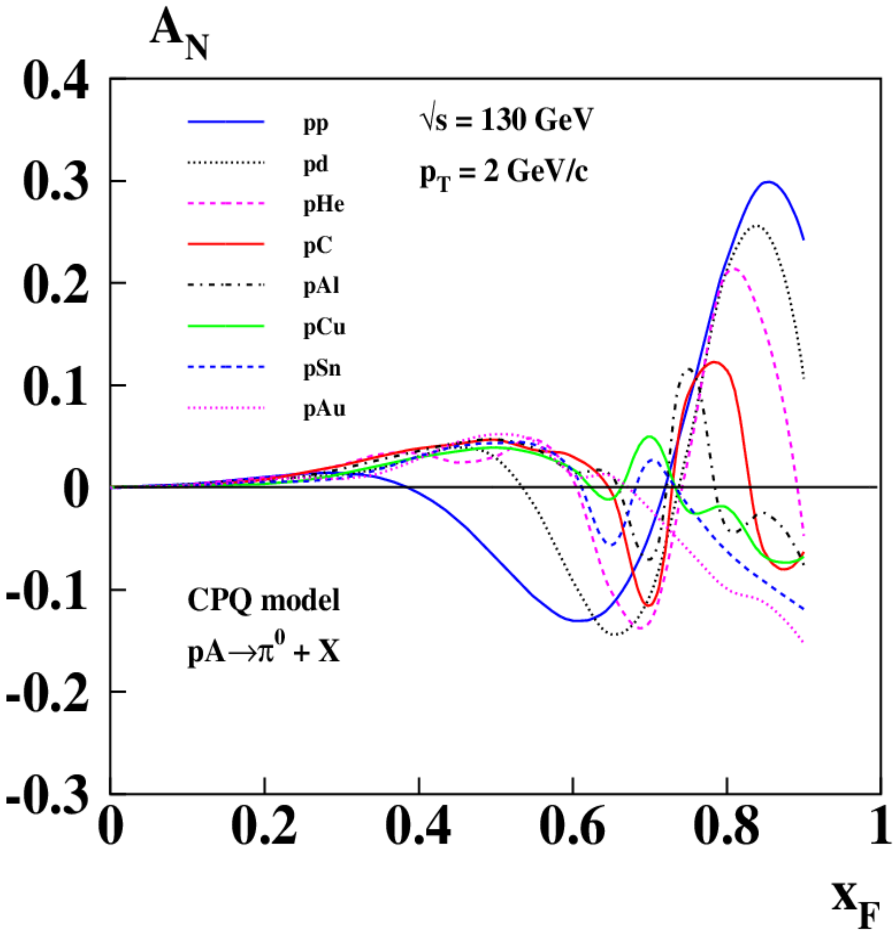

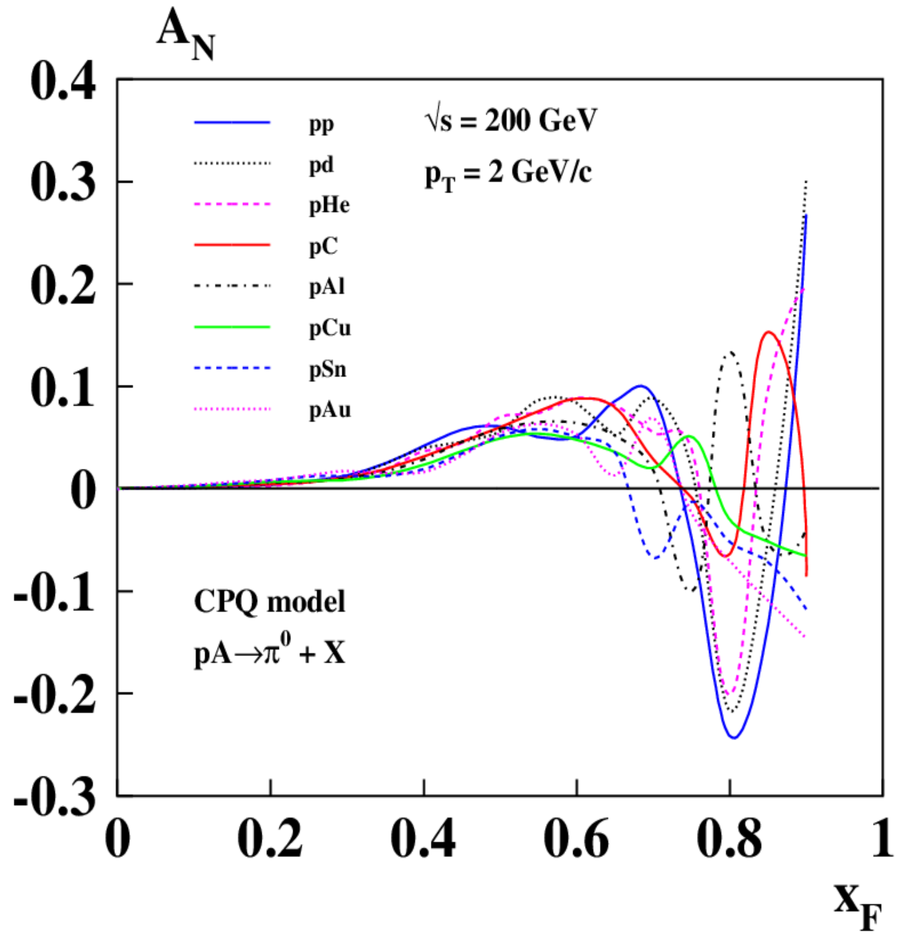

Fig. 13. Calculations of the dependence of A_N on x_F at energy $\sqrt{s} = 130$ GeV, $p_T = 2$ GeV/c, in pA collisions.

Fig. 14. Calculations of the dependence of A_N on x_F at energy $\sqrt{s} = 200$ GeV, $p_T = 2$ GeV / c, in pA collisions.

Oscillation of $A_N(x_F)$ in a strong chromomagnetic field at 130 GeV and 200 GeV.

Predictions on $A_N(x_F, p_T)$ for $p\uparrow + p(A) \rightarrow \pi^0 + X$

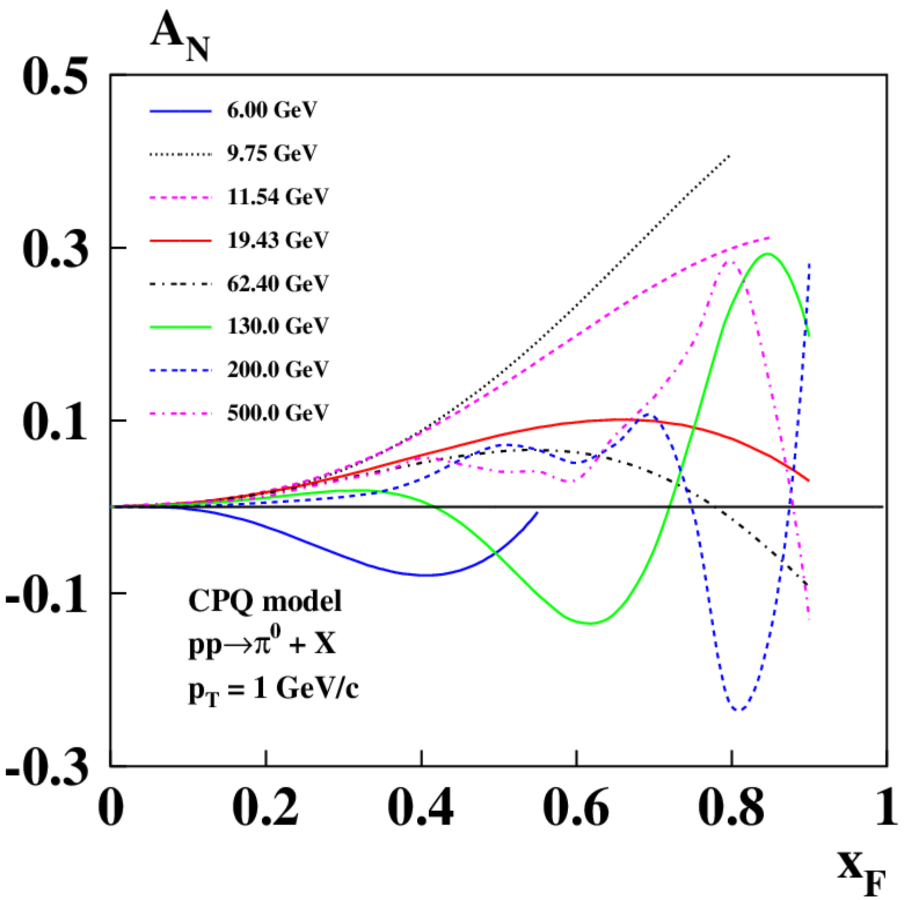

Fig. 15. Calculations of the dependence of A_N on x_F at several values of energy $\sqrt{s}$, p_T = 1 GeV/c, in pp collisions.

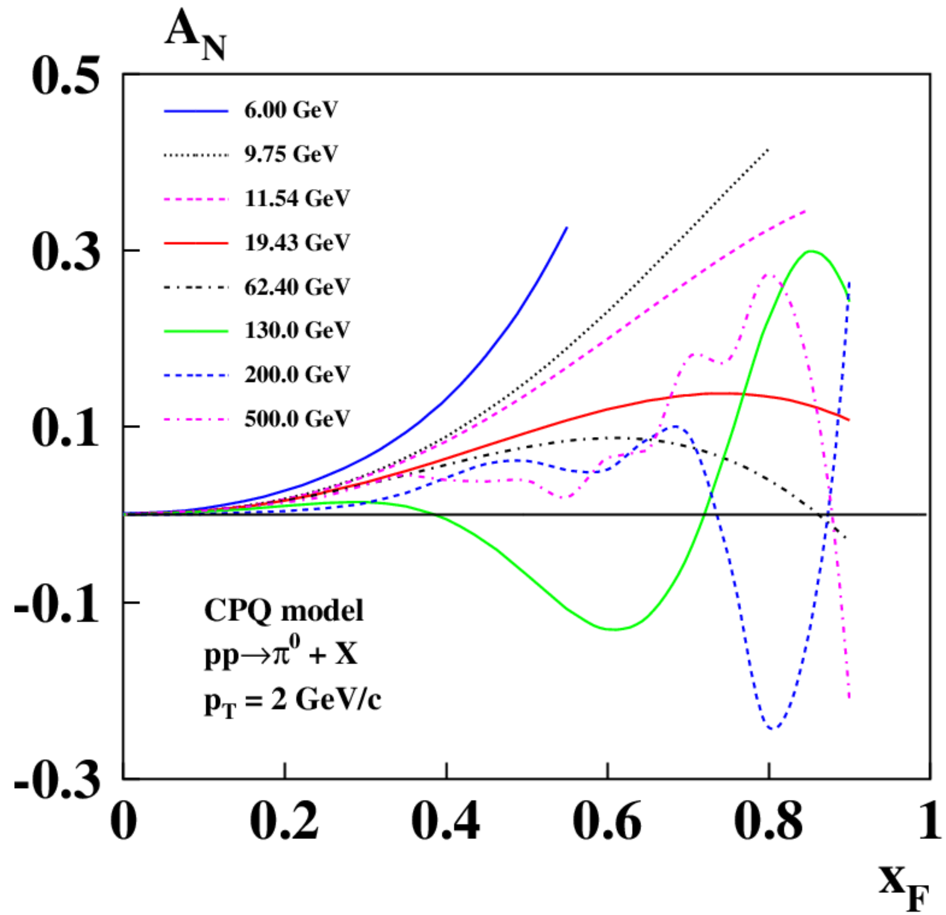

Fig. 16. Calculations of the dependence of A_N on x_F at several energies $\sqrt{s}$, p_T = 2 GeV/c, in pp collisions.

Oscillation of $A_N(x_F)$ in a strong chromomagnetic field at 130 GeV and 200 GeV.
Change of A_N sign for $\sqrt{s}$ = 6 GeV with p_T increasing.

References

[1] Abramov V.V. Phenomenology of single-spin effects in hadron production at high energies // Phys. Atom. Nucl. — 2009. — V. **72**, no. 11. — P. 1872–1888.
[2] V.V. Abramov, A. Aleshko, V.A. Baskov, E. Boos, V. Bunichev et al., e-Print: 2102.08477 [hep-ph], JINR preprint E2-2021-12.
[3] N.I.Kochelev, Phys.Lett. **B426**(1998) 149.
[4] Y.Pan, *Int.J.Mod.Phys.Conf.Ser.* **40** (2016) 01, 1660037.
[5] B.I.Abelev et al. Phys.Rev.Lett.**101**(2008) 222001.
[6] C.Dilks for STAR Collab., *PoS* DIS2016 (2016) 212, e-Print: 1805.08875[hep-ex].
[7] V.V. Abramov et al., Phys. Atom. Nucl.**77**(2014) 595-601.
[8] D.L. Adams et al., Z.Phys. **C56**(1992)181-184.
[9] S.Heppelmann et al., arXiv:0905.2840v1 [nucl-ex].
[10] A.Adare et al., Phys. Rev. **D90** (2014) 1, 012006, e-Print:1312.19995[hep-ex].
[11] L. Adamczyk et al., Phys.Rev. **D86** (2012) 051101.
[12] L. Adamczyk et al., Phys. Rev. **D89** (2014) 1, 012001.
[13] L.Nogach, AIP Conf. Proc. **915**(2007) 543-546. hep-ex/0612030 [hep-ex].
[14] M.H.Kim et al., Phys. Rev. Lett. **124**(2020) 252501.
[15] Baranov S.P. On the production of doubly flavored baryons in p p, e p and gamma gamma collisions // Phys. Rev. — 1996. — V. **D54** — P. 3228–3236.

Conclusions and outlook

Analysis of the available data and calculations performed using the CPQ model in areas not yet investigated indicate the possible presence of a number of features in the dependences on kinematic variables and target atomic weight.

1) Oscillation of $A_N(x_F)$ with negative $A_N(x_F)$ sign for $0.5 \leq x_F \leq 0.7$ is expected at energies around $\sqrt{s} = 130$ GeV.

This effect can be studied at the RHIC collider (BNL).

2) A significant positive value of A_N is expected at energies around $\sqrt{s} = 9$ GeV and large $x_F \geq 0.5$. A strong A-dependence of A_N is expected in this area. On heavy nuclei A_N is expected to be negative in this case.

This effect can be studied at the NRC Kurchatov Institute - IHEP (using the SPASCHARM facility) and at the NICA collider at JINR (using the SPD facility).

Thank you for attention!

BACKUP SLIDES

The role of color factor λ

When taking into account the interaction of a test quark with the field created by a moving spectator quark, it is necessary to take into account the color factor for the corresponding pair of quarks (spectator and test quarks). An analysis of the data have shown that the quark-antiquark pair interacts predominantly in the color-singlet state with the color factor $\mathbf{C_F = 4/3}$, and the quark-quark or antiquark-antiquark pair interacts in the color-antitriplet state with $\mathbf{C_F = 2/3}$. For a hydrogen-like potential, the wave function of two quarks or a quark and an antiquark at zero coordinate is proportional to $|\Psi(0)| \sim (C_F \alpha_S)^{3/2}$ [3], which leads to the ratio of contributions from qq and $q\tilde{q}$ interactions to ν_A of the order

$$\lambda \approx -|\Psi qq(0)|^2/|\Psi q\tilde{q}(0)|^2 = -1/8. \qquad (1)$$

The minus sign in (1) takes into account the opposite sign of the field created by a moving spectator quark and a moving spectator antiquark. Experimentally, the value of the global parameter **λ**, obtained as a result of the global fit of the polarization data, turned out to be $\mathbf{\lambda = -0.1363 \pm 0.0003}$. A value, more close to the experimental one is given by the formula $\lambda = 1 - \exp(1/8) \approx -0.1331$, which can be considered as a generalization of formula (1).

[15] Baranov S.P. On the production of doubly flavored baryons in p p, e p and gamma gamma collisions // Phys. Rev. — 1996. — V. D54 — P. 3228–3236.

Effective number of nucleons in the target (A_{eff}) in the case of hA collisions

The effective number of nucleons in the target nucleus is equal to their number in a tube of radius $R_b = r_0 A_b^{1/3}$:

$$A_{eff} = A_2\{1 - [1 - (A_b/A_2)^{2/3}]^{3/2}\} \approx 0.69 A_2^{1/3}. \qquad (4)$$

If $A_2 < A_b$, then $A_{eff} = A_2$. For nucleon target, $A_{eff} = 1$.

A_b is the free model parameter obtained from the global fit of 87 inclusive single-spin reactions.

Fit: $A_b = 0.314 \pm 0.006$; $R_b = r_0 A_b^{1/3} \approx 0.82 \pm 0.02$ fm, (5)

where A_2 – target nucleus atomic weight, $r_0 = 1.2$ fm.

For an incident hadron or lepton, we set $A_1 = 1$.

Equations for A_N, P_N and $(\rho_{00}$-1/3)

$P_N \approx C(\sqrt{s})\, F(p_T, A)[G(\varphi_A) - \sigma G(\varphi_B)\,]$, (3)

$G(\varphi_A) = [1 - \cos\varphi_A]/\varphi_A + \varepsilon\varphi_A$, spin precession and S-G force, (4)

where $\varepsilon = -0.00497 \pm 0.00009$ - global, σ – local parameter.

$C(\sqrt{s}) = v_0/[(1 - E_R/\sqrt{s})^2 + \delta_R{}^2]^{1/2}$, spin precession vs E_Q (5)

$F(p_T,A) = \{1 - \exp[-(p_T/p^0{}_T)^{2.5}\,]\}(1 - \alpha_A \ln A)$, color form factor (6)

$v_0 = -D_r\, g^a{}_Q\, P_Q / 2(g^a{}_Q - 2)$, sign and magnitude of A_N and P_N (7)

$\varphi_A = \omega^0{}_A y_A$, $\varphi_B = \omega^0{}_B y_B$, integral “precession angles” (8)

$y_A = x_A - (E_0/\sqrt{s} + f_0)[1 + \cos\theta_{cm}\,] + a_0[1 - \cos\theta_{cm}\,]$, (9)

$y_B = x_B - (E_0/\sqrt{s} + f_0)[1 - \cos\theta_{cm}\,] + a_0[1 + \cos\theta_{cm}\,]$, (10)

$x_A = (x_R + x_F)/2$, $x_B = (x_R - x_F)/2$. scaling variables (11)

$\omega^0{}_{A(B)} = g_s \alpha_s \nu_{A(B)}\, m_r (g^a{}_Q - 2)/M_Q$, $m_r = 0.2942 \pm 0.0072$ GeV. (12)

$\nu_{A(B)}$ - effective contributions of the spectator quarks to the field B^a.

Oscillation of A_N and P_N in a strong color field

$$P_N \approx C(\sqrt{s})\, F(p_T, A)[G(\varphi_A) - \sigma G(\varphi_B)\,], \qquad (3)$$

$$G(\varphi_A) = [1 - \cos\varphi_A]/\varphi_A + \varepsilon\varphi_A,$$ is a result of the spin precession and S-G force (4)

were φ_A, φ_B – are the integral "spin precession angles" in the fragmentation regions of the projectile A and the target B, respectively. $\varepsilon = -0.00497 \pm 0.00009$.
Analysis shows that effective length S of the field $\mathbf{B}^a$ is: $S_0 x_A$ or $S_0 x_B$ for fragmentation regions of colliding particles A and B, where S_0 is about 1 fm.

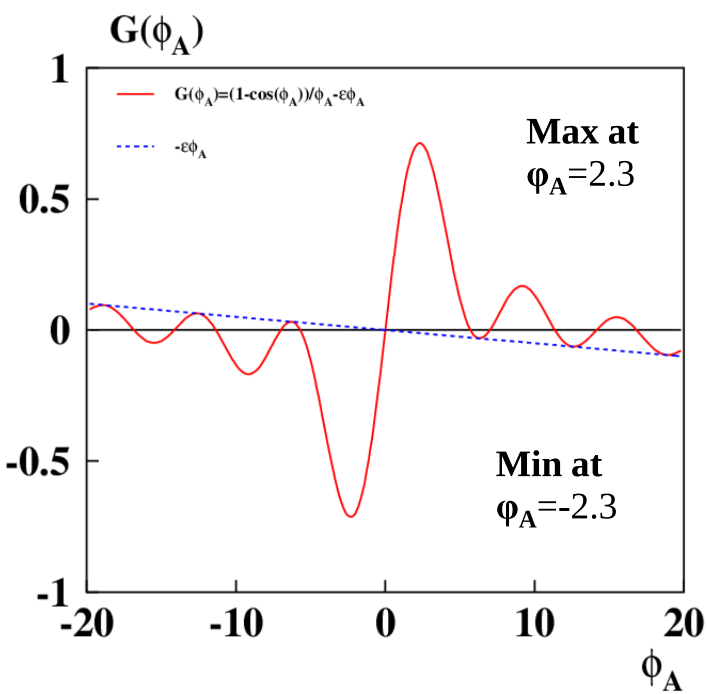

$$\varphi_A = \omega^0{}_A y_A, \quad \varphi_B = \omega^0{}_B y_B\,; \qquad (8)$$

$$\omega^0{}_{A(B)} = g_s \alpha_s \nu_{A(B)}\, m_r (g^a{}_Q - 2)/M_Q\,, \qquad (12)$$

$$m_r = 0.2942 \pm 0.0072 \text{ GeV}; \quad \alpha_s = g_s{}^2/4\pi;$$

$$y_A = x_A - (E_0/\sqrt{s} + f_0)[1 + \cos\theta_{cm}] + a_0[1 - \cos\theta_{cm}] \quad (9)$$

$$y_B = x_B - (E_0/\sqrt{s} + f_0)[1 - \cos\theta_{cm}] + a_0[1 + \cos\theta_{cm}] \quad (10)$$

$x_A = (x_R + x_F)/2$, $x_B = (x_R - x_F)/2$ - scaling variables. (11)

$\nu_{A(B)}$ - effective contributions of the spectator quarks to the field $\mathbf{B}^a$.

Quark counting rules for ν_A $(A + B \to C + X)$

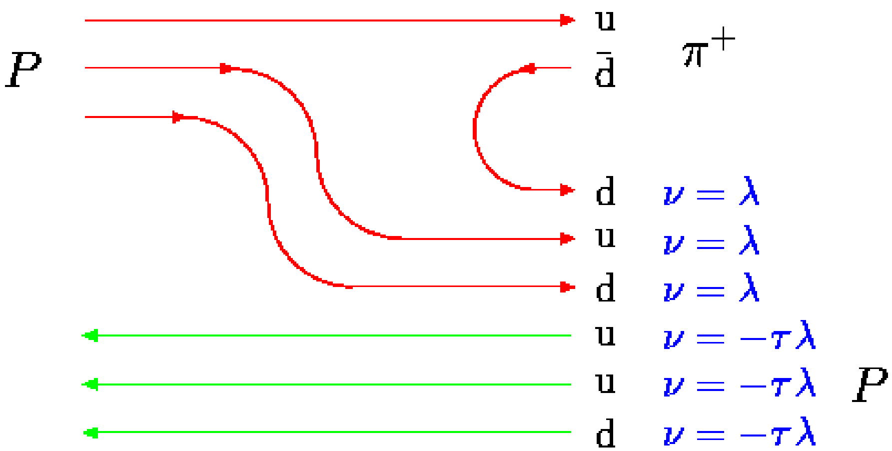

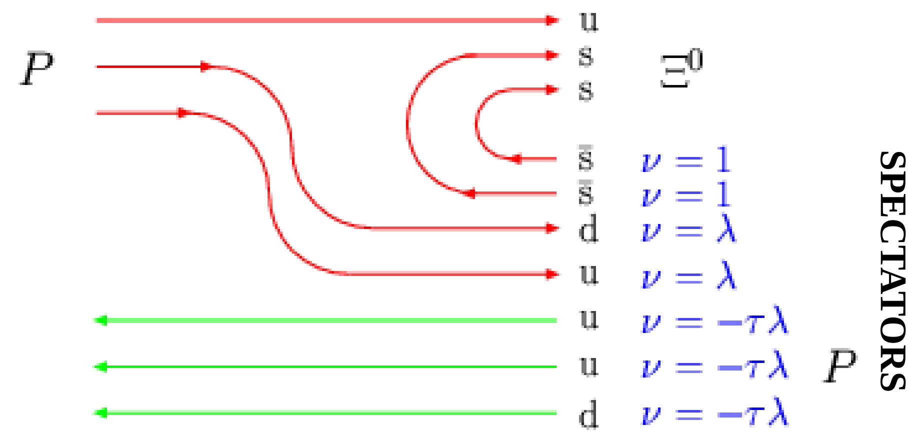

$\int \mathbf{E}^a \sim \int \mathbf{B}^a \sim \nu_A = [3\lambda - 3\tau\lambda] < 0;$ $\quad \int \mathbf{E}^a \sim \int \mathbf{B}^a \sim \nu_A = [2 + 2\lambda - 3\tau\lambda] > 0$

$\mathbf{A_N \sim P_U \nu_A (g^a_U - 2)/2M_U > 0;}$ $\quad \mathbf{P_N \sim \nu_A (g^a_S - 2)/2M_S < 0.}$

qq, $\tilde{q}\tilde{q}$ -SU(3)$_c$ antitriplet, weight $\nu = \lambda$; $\quad C_F = 2/3$ – color factor

$q\tilde{q}$, $\tilde{q}q$ -SU(3)$_c$ singlet, weight $\nu = 1$. $\quad C_F = 4/3$ – color factor

- S.P. Baranov, Phys. Rev. D54, 3228 (1996). $\quad |\psi|^2 \sim (C_F \alpha_S)^3$. (16)
- $\lambda = -|\psi_{qq}(0)|^2 / |\psi_{q\tilde{q}}(0)|^2 \approx 1 - e^{1/8} \approx -0.1332$ **color factor** (17)
- **$\lambda = -0.1363 \pm 0.0003$, $\tau = 0.0267 \pm 0.0012$, fit for 85 reactions.**

Quark counting rules for $p\uparrow + p \rightarrow \pi^+ + X$

$\nu_A = 3\lambda - 3\tau\lambda = -0.398$ (3)

$\nu_B = \nu_A$, where global parameters for 85 (3608 points) reactions are:

$\lambda = -0.1363 \pm 0.0003$, (4)

$\tau = 0.0267 \pm 0.0005$. (5)

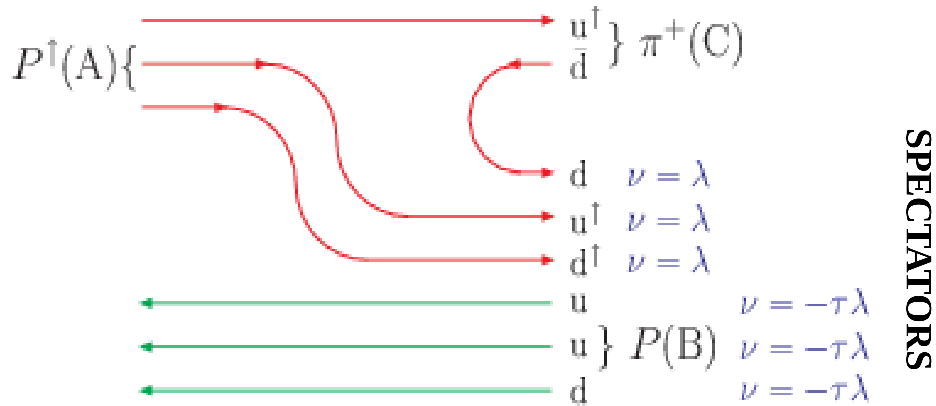

For comparison is shown a quark flow in reaction $p\uparrow + p \rightarrow p + X$.

The effective number of quarks is:

$\nu_A = 2 + 2\lambda - 3\tau\lambda = 1.738$, (6)

$\nu_B = \nu_A$.

and $p\uparrow + p \rightarrow p + X$

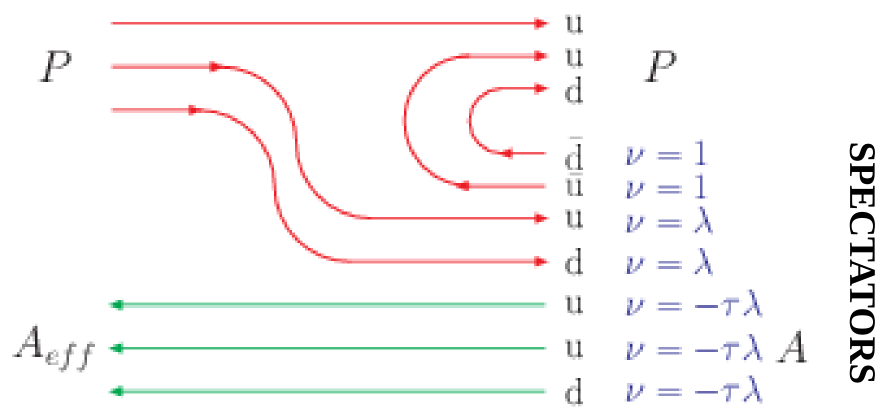

So, in case of reaction $p\uparrow + p \rightarrow p + X$ ν_A is approximately 4 times higher, than in case of $p + p \rightarrow \pi^+ + X$. As a result, $A_N(x_F)$ should oscillates with approximately 4 times higher frequency for $p\uparrow + p \rightarrow p + X$ reaction. The sign **($-g_S\nu_A P_Q$)** of A_N for proton must be opposite (negative) at small x_F.

Quark flow diagrams for the cascade antihyperon production

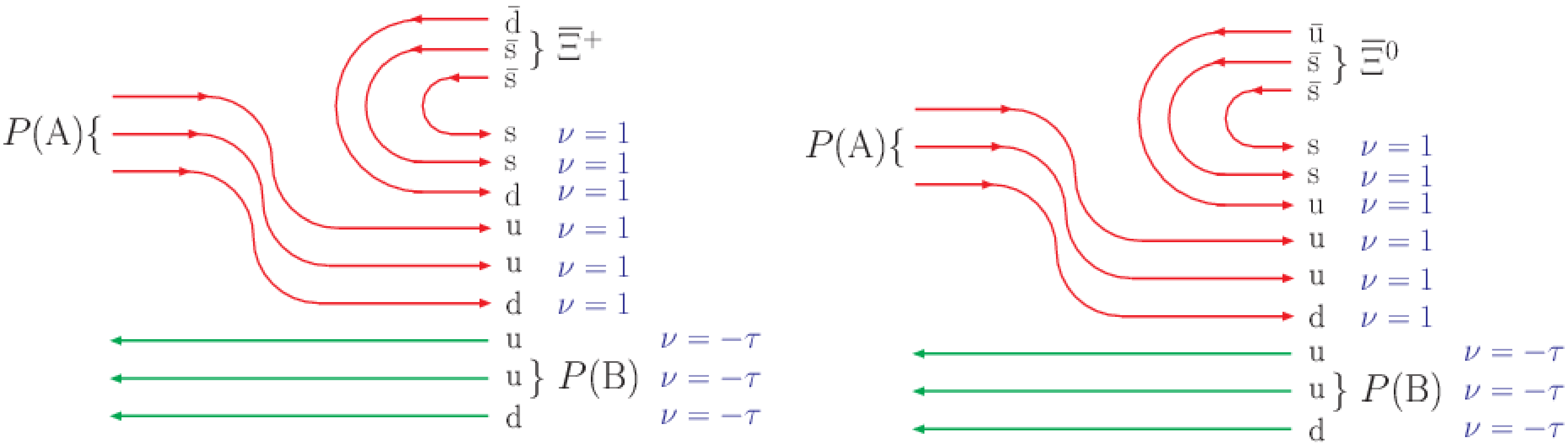

In case of $\bar{\Xi}^+$ and $\bar{\Xi}^0$ production in pA-collisions the quark flow diagrams look similar. But constituent masses of u and d are different.

Six spectator quarks interact with each of active valence test quark of antihyperon and create a very strong chomomagnetic field.

Large values of $\nu_A = \nu_B = 6 - 3\tau$ leads to a very high quark spin precession frequency and the corresponding high oscillation frequency $\boldsymbol{\omega^0_{A(B)}}$ for $P_N(x_F)$, which is proportional to ν_A or ν_B.

Quark counting rules for the p + p → Ξ⁻ + X

$\nu_A = (2 + 2\lambda) - 3\tau\lambda = 1.738$ (3)

$\nu_B = \nu_A$, where global parameters for 85 reactions are:

$\lambda = -0.1363 \pm 0.0003$,

$\tau = 0.0267 \pm 0.0005$.

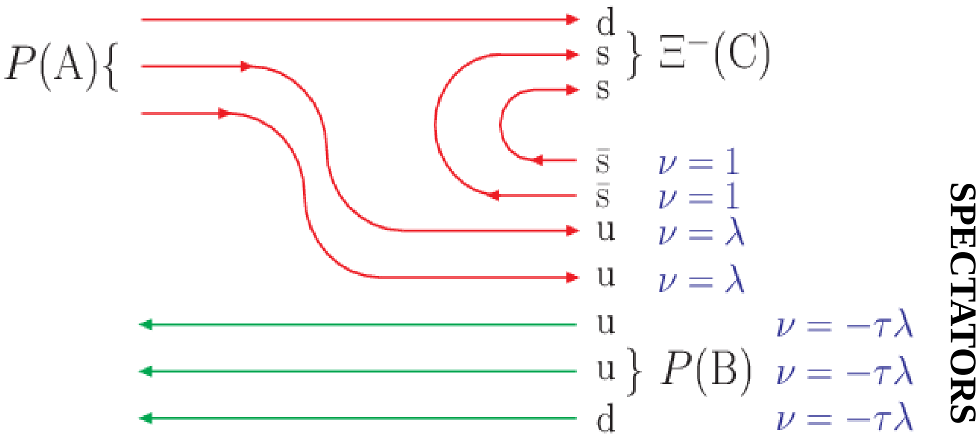

For comparison is shown a quark flow in reaction p + p → Λ + X.

The effective number of quarks is:

$\nu_A = (1 + \lambda) - 3\tau\lambda = 0.8746$ (4)

$\nu_B = \nu_A$.

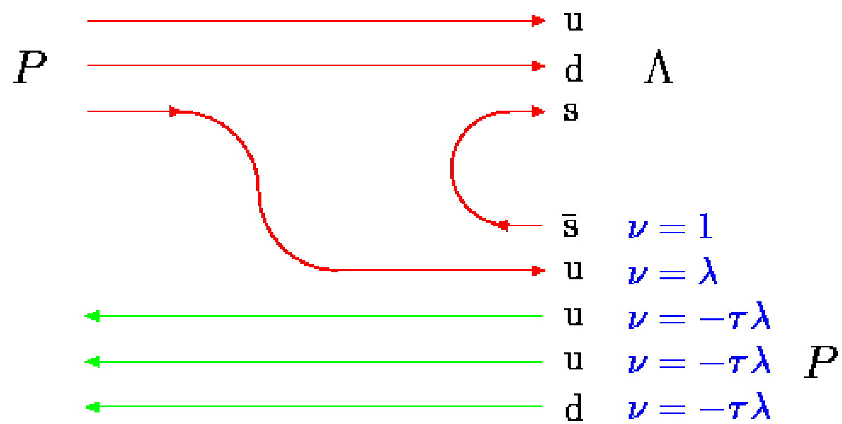

$pp \to \Lambda + X$ production quark diagram.

Color flux tube counting.

So, in case of reaction p + p → Ξ⁻ + X ν_A is approximately two times higher, than in case of p + p → Λ + X.

As a result, $P_N(x_F)$ should oscillates with approximately two times higher frequency for p + p → Ξ⁻ + X reaction.

Model parameters (global and local)

1) m_s = 98±2 MeV; 2) m_c = 1264±17 MeV; 3) $\Delta\mu^a{}_u$ = -0.4839±0.0017;

4) ΔM_u = 0.2665±0.0012; 5) ΔM_d = 0.3033±0.0013; 6) ΔM_s = 0.3703±0.0020;

7) τ = 0.0267 ±0.0005; 8) λ = -0.1363 ±0.0003; 9) ε = -0.00497±0.00009;

10) W_0=275.6 ±1.3 GeV; 11) P_N = 84.7 ± 0.4 GeV; 12) m_r = 0.3573±0.0016 GeV;

13) n_q = 4.671±0.018; 14) A_a = 10.35±0.55; 15) A_b= 0.3084±0.0012;

16) A_T = 59.6±5.8; 17) δ_R = 0.2907±0.0026; 18) a_f = 3.092±0.047;

19) V_T = 0.1437±0.062; 20) p_m = 0.152±0.038 GeV; 21) a_{81} = 1.622±0.050;

22) a_{56} = 0.4220±0.0013 GeV; 23) E_0 = -83.8±0.4 GeV; 23) a_{51}=0.0236±0.0015;

25) E_c = 0.000511±0.000003; 26) a_{41}=0.1428±0.0013; 27) η = -1.761±1.18;

$W_0 \approx m_p^2/m_q \approx 255 \pm 24$ GeV; $m_q \approx (m_u+m_d)/2 \approx 3.45 \pm 0.33$MeV; $\lambda \approx 1-\exp(1/8) \approx -0.133$;

Global Data Analysis: A_N

Inclusive reactions, in which was measured single-spin asymmetry in hadron-hadron collisions (26 reactions).

№	Reaction	№	Reaction	№	Reaction
1	$p^\uparrow p(A) \to \pi^+$	10	$p^\uparrow A \to J/\psi^\uparrow$	19	$\pi^+ p^\uparrow \to \pi^+$
2	$p^\uparrow p(A) \to \pi^-$	11	$p^\uparrow p \to \eta$	20	$\pi^- p^\uparrow \to \pi^-$
3	$p^\uparrow p \to \pi^0$	12	$d^\uparrow A \to \pi^+$	21	$\pi^- p^\uparrow \to \pi^0$
4	$p^\uparrow p(A) \to K^+$	13	$d^\uparrow A \to \pi^-$	22	$\pi^- d^\uparrow \to \pi^0$
5	$p^\uparrow p(A) \to K^-$	14	$\tilde{p}^\uparrow p \to \pi^+$	23	$K^- d^\uparrow \to \pi^0$
6	$p^\uparrow p \to K^0_S$	15	$\tilde{p}^\uparrow p \to \pi^-$	24	$K^- p^\uparrow \to \pi^0$
7	$p^\uparrow p(A) \to n$	16	$\tilde{p}^\uparrow p \to \pi^0$	25	$\pi^- p^\uparrow \to \eta$
8	$p^\uparrow p(A) \to p$	17	$\tilde{p}^\uparrow p \to \eta$	26	$\tilde{p}\, p^\uparrow \to \pi^0$
9	$p^\uparrow A \to \tilde{p}$	18	$\tilde{p}\, d^\uparrow \to \pi^0$		

Global Data Analysis: P_N

Inclusive reactions, in which was measured hyperon polarization in hadron-hadron collisions (31 reactions).

№	Reaction	№	Reaction	№	Reaction
27	$p\,p(A) \rightarrow \Lambda^{\uparrow}$	37	$\Sigma^{-} A \rightarrow \Sigma^{+\uparrow}$	48	$K^{-} p \rightarrow \Lambda^{\uparrow}$
28	$p\,A \rightarrow \Xi^{-\uparrow}$	38	$\Sigma^{-} A \rightarrow \Xi^{-\uparrow}$	49	$K^{-} A \rightarrow \Xi^{-\uparrow}$
29	$p\,A \rightarrow \Xi^{0\uparrow}$	39	$p\,A \rightarrow \tilde{\Lambda}^{\uparrow}$	50	$\pi^{-} A \rightarrow \Xi^{-\uparrow}$
30	$p\,A \rightarrow \Sigma^{+\uparrow}$	40	$\Sigma^{-} A \rightarrow \tilde{\Lambda}^{\uparrow}$	51	$\pi^{+} p \rightarrow \Lambda^{\uparrow}$
31	$p\,p \rightarrow p^{\uparrow}$	41	$p\,A \rightarrow \tilde{\Xi}^{+\uparrow}$	52	$K^{+} p \rightarrow \Lambda^{\uparrow}$
32	$p\,A \rightarrow \Sigma^{-\uparrow}$	42	$p\,A \rightarrow \tilde{\Xi}^{0\uparrow}$	53	$\pi^{-} p \rightarrow \Lambda^{\uparrow}$
33	$p\,A \rightarrow \Omega^{-\uparrow}$	43	$p\,A \rightarrow \tilde{\Sigma}^{-\uparrow}$	54	$K^{+} p \rightarrow \tilde{\Lambda}^{\uparrow}$
34	$\Sigma^{-} A \rightarrow \Lambda^{\uparrow}$	44	$\tilde{p}\,A \rightarrow \tilde{\Lambda}^{\uparrow}$	55	$\pi^{-} p \rightarrow \tilde{\Lambda}^{\uparrow}$
35	$p\,A \rightarrow \Sigma^{0\uparrow}$	45	$A_1+A_2 \rightarrow \Lambda^{\uparrow}$	56	$K^{-} p \rightarrow \tilde{\Lambda}^{\uparrow}$
36	$\Lambda\,A \rightarrow \Omega^{-\uparrow}$	46	$Au+Au \rightarrow \Lambda^{\uparrow(Glob)}$	57	$\pi^{-} A \rightarrow \tilde{\Xi}^{+\uparrow}$
		47	$Au+Au \rightarrow \tilde{\Lambda}^{\uparrow(GloB)}$		

Global Data Analysis: A_N, P_N, ρ_{00}

Other inclusive reactions, in which was measured vector meson polarization and lepton induced reactions (24 reactions).

№	Reaction	№	Reaction	№	Reaction
58	$p\ A \to J/\psi^{\uparrow}$	67	$n\ A \to K^{*}(892)^{-\uparrow}$	73	$e^{+}\ A \to \Lambda^{\uparrow}$
59	$\tilde{p}\ A \to J/\psi^{\uparrow}$	68	$n\ A \to K^{*}(892)^{+\uparrow}$	74	$e^{+}\ A \to \tilde{\Lambda}^{\uparrow}$
60	$p\ A \to Y(1S)^{\uparrow}$	69	$p\ p \to \varphi(1020)^{\uparrow}$	75	$e^{+}\ p^{\uparrow} \to \pi^{+}$
61	$p\ A \to Y(2S)^{\uparrow}$	70	$\tilde{p}\ p \to \rho(770)^{\uparrow}$	76	$e^{+}\ p^{\uparrow} \to \pi^{-}$
62	$p\ p \to Y(1S)^{\uparrow(\tilde{\lambda})}$	71	$AuAu \to \tilde{K}^{*}(892)^{0\uparrow}$	77	$e^{+}\ p^{\uparrow} \to K^{+}$
63	$p\ p \to Y(2S)^{\uparrow(\tilde{\lambda})}$	72	$AuAu \to \varphi(1020)^{\uparrow}$	78	$e^{+}\ p^{\uparrow} \to K^{-}$
64	$p\ p \to Y(3S)^{\uparrow(\tilde{\lambda})}$			79	$\mu^{-}\ 6LiD^{\uparrow} \to h^{+}$
65	$\tilde{p}\ p \to Y(1S)^{\uparrow}$			80	$\mu^{-}\ 6LiD^{\uparrow} \to h^{-}$
66	$\tilde{p}\ p \to Y(2S)^{\uparrow}$			81	$\nu_{\mu}\ A \to \Lambda^{\uparrow}$